Launch and Assembly

Once on-orbit the modular elements would be attached end to end. At the front and aft ends of each element are interfaces where propellant, gas pressurant, communication, and power lines would be joined. All subsystems, propellant lines, etc. are preintegrated and located on the structural truss to which the tank is attached. Positioned above the truss are one or more remote manipulator system (RMS) arm units that can transverse the length of the truss for the purpose of joining sections together. RMS units traveling across the truss top have access to these subsystems for joining, inspection, repair, or change out; they could accommodate suited personnel to facilitate these operations if required. Assembly consists of attaching the common tank/truss elements at their end-to-end interconnect points as shown in Fig. 4. Rather than sending up to orbit a separate platform prior to the delivery of the spacecraft components, a RMS operates from the first element delivered to orbit. The forward habitat/truss element segment acts as the assembly platform for the remaining elements. Utilizing its RCS, the forward element would translate to within RMS arm capture distance of the second coorbiting element. Moving along the top rails of the rigid truss section, the autonomous (or crew-assisted) RMS would capture and pull to an aligned position the second element and connect the two at their end-to-end interconnects. In addition to the structural connection of the truss sections, this first interface would connect communication and power lines. Once joined, secured, and inspected, the RMS would then move onto the second element, travel the length of its truss rail, reaching the unconnected end where again the RCS would be used to maneuver the two connected modules near enough to the third element to repeat the capture and connection process. For the second-to-third element connection the interface consists of propellant and gas pressurant line quick-connect devices in addition to power and communication connections. This process is repeated for the fourth, aft element, completing the assembly. The number of connection operations would always be one less than the number of elements delivered to orbit; i.e., for a four-element Mars vehicle, three capture operations would be required, and for a three-element Lunar vehicle, two would be required. Furthermore, once the vehicle has completed a mission and returned to Earth orbit, its two reusable core elements (habitat and propulsion) could be rejoined to new noncore tankage modules and a new landing craft on-orbit, allowing for the economical second use of the expensive habitat and propulsion modules.[22]

Conclusion

After five years of detailed study, this phase 3 configuration became the preferred vehicle type for human Mars missions because of its modular design, ease of launch vehicle packagability, ease of on-orbit assembly, and minimal reassembly requirements for subsequent reuse.

Acknowledgment

Work reported in this Note was performed for the NASA Marshall Space Flight Center under Contract NAS8-37857.

References

[1]"Integrated Manned Interplanetary Spacecraft Concept Definition Study," The Boeing Co., Vol. IV System Definition, Final Rept. D2-113544-4, NAS1-6774, Seattle, WA, Jan. 1968.

[2]"Modular Vehicle Study," Lockheed, NAS8-20007, Sunnyvale, CA, 1965.

[3]"Manned Mars Mission Study," TRW, NAS2-1409, Redondo Beach, CA, March 1965.

[4]"Manned Mars Exploration in the Unfavorable (1975–1985) Time Period," Douglas Aircraft, Rept. SM-45575 (NAS8-11005), Santa Monica, CA, Jan. 1964.

[5]"Manned Mars and Venus Exploration Study," General Dynamics/Convair, Rept. AOK 65-002-1 (NAS8-11327), San Diego, CA, June 1965.

[6]"Manned Mars and/or Venus Flyby Vehicle Systems Study," North American Aviation, NAS9-3499, Seal Beach, CA, June 1965.

[7]Kraemer, R., and Larson, V., "Comparison of Several Propulsion Systems for a Mars Mission," Rocketdyne, Aviation Conf., ASME Paper 59-AV-46, Los Angeles, 1959.

[8]"EMPIRE—A Study of Early Manned Interplanetary Missions," Philco-Ford, NAS8-5025, Newport Beach, CA, Nov. 1962.

[9]Seifert, H. S., and Mills, M. M., "Problems in the Application of Nuclear Energy to Rocket Propulsion," *Physical Review*, Vol. 71, 1947, p. 279.

[10]Shepherd, L. R., and Cleaver, A. V., "The Atomic Rocket," *Journal of the British Interplanetary Society*, Vol. 7, Nos. 5, 6, 1948; Vol. 8, Jan. 1949, pp. 23, 24, 30–37.

[11]von Braun, W., *Das Marsprojekt*, 1949.

[12]Ehricke, K. A., Whitlock, C. M., Chapman, R. L., and Purdy, C. H., "Calculations on a Manned Nuclear Propelled Space Ship," American Rocket Society, Paper 352-57, 1957.

[13]"America's Next Decades in Space," NASA, Rept. for the Space Task Group, Washington, DC, Sept. 1969.

[14]"Hearing Before the Committee on Aeronautical and Space Sciences," U.S. Senate, 91st Congress, First Session, Aug. 1969.

[15]Bellcomm, Inc., "Long Range Space Program Planning," NASA, Contract NASW-417, TR-69-105-2-1, Oct. 1969.

[16]"Nuclear Flight Systems Definition Study," Lockheed Missiles and Space Co., NAS8-24715, Sunnyvale, CA, 1970.

[17]"Space Transfer Concepts and Analysis for Exploration Missions," The Boeing Co., Phase I Final Rept., NAS8-37857, Huntsville, AL, March 1991.

[18]Stafford, T., "America at the Threshold: Report of the Synthesis Group on America's Space Exploration Initiative," National Space Council, Arlington, VA, May 1991.

[19]"Space Transfer Concepts and Analysis for Exploration Missions," The Boeing Co., Fourth Quarterly Review Rept., NAS8-37857, Huntsville, AL, Oct. 1990.

[20]Venetokis, P., and Nelson, C., "Pluto Exploration Strategies Enabled by SNTP Technology," AIAA Paper 93-1951, June 1993.

[21]Donahue, B., "Mars Ascent-Stage Design Utilizing Nuclear Propulsion," *Journal of Spacecraft and Rockets*, Vol. 32, No. 3, 1995, pp. 552–558.

[22]Donahue, B., "Human Mars Missions: Cost Driven Architecture Assessments," AIAA Paper 98-5285, Oct. 1998.

I. E. Vas
Associate Editor

Effects of Shock Wave Impingement on Supersonic Film Cooling

Kenichi Takita* and Goro Masuya†
Tohoku University, Sendai 980-8579, Japan

Introduction

FILM cooling, especially in combination with regenerative cooling, is a promising way to protect the engine wall of a scramjet. The effect of the interaction between a shock wave and a coolant flow on cooling efficiency becomes important in supersonic flow. Therefore, many experiments[1–3] on such interactions have been conducted recently. Compared with the case without shock impingement, however, theoretical or numerical studies on film cooling with shock impingement have been insufficient, and so the mechanism of the interaction and the degree of its influence on the cooling efficiency are not well understood. To increase understanding, the effect of shock impingement on film cooling and the change of the flowfield were numerically investigated. Moreover, the effect of an increase in the injection Mach number of the coolant was investigated as a way to reduce its influence.

Numerical Method

Two-dimensional compressible Navier–Stokes equations in generalized curvilinear coordinates for multispecies were solved with a k-ε low Reynolds number turbulent model[4] in which the eddy viscosity did not become zero when flow separation occurred.

Received 18 May 1998; revision received 5 March 1999; accepted for publication 20 March 1999. Copyright © 1999 by the American Institute of Aeronautics and Astronautics, Inc. All rights reserved.

*Research Associate, Department of Aeronautics and Space Engineering. Member AIAA.

†Professor, Department of Aeronautics and Space Engineering. Member AIAA.

Compressibility effect terms were added to the k equation. The third-order MUSCL total variation diminishing scheme for convective terms and a second-order central difference scheme for viscous terms were used for the finite difference.

The configuration of the flowfield was similar to the equipment of Kanda et al.[2] and Kanda and Ono[3] to compare the calculation with their shock impingement experimental data. The flowfield was composed of a main flow and a coolant flow separated by a 1.5-mm-thick splitter plate. The height of the coolant injector, d_{inj}, was 4 mm. The shock generator, with a deflection angle of 6 deg, was attached to the upper wall. The computational grid, which was concentrated near the wall, had 499 × 111 grid points. Boundary-layer profiles for both flows were deduced from the $\frac{1}{7}$th power law.

Results and Discussion

Comparison with Experiments

The present numerical simulation was first compared with experimental data obtained by Kanda et al.[2] to evaluate its validity. Inflow conditions were matched to those of the experiment, where total pressure P_0, total temperaure T_0, Mach number M, and boundary-layer thickness δ were 1350 kPa, 280 K, 2.35, and 5.0 mm for the main flow (denoted by subscript m) and were 200 kPa, 230 K, 1.0, and 1.0 mm for the coolant flow (denoted by subscript c), respectively. Both of the flows were nitrogen. Because turbulent kinetic energy k was not measured in the experiment, its value at the inflow boundary was assumed to be 0.15% of the kinetic energy of the main flow. Parametric calculations of the value of turbulent kinetic energy from 0.15 to 1.5% for the main flow showed that it had little effect on the characteristics of film cooling.

The film cooling efficiency f_c is defined as follows:

$$f_c = \frac{T_{aw} - T_{rm}}{T_{rc} - T_{rm}} \tag{1}$$

where T_{aw} is local adiabatic wall temperature and T_r is adiabatic recovery temperature calculated by using the inflow conditions and the assumption that the recovery factor is 0.9.

Figure 1 shows comparisons with the Ref. 2 experiment for no shock impingement on wall pressure (Fig. 1a) and for film cooling efficiency (Fig. 1b). The approximate relation obtained from the numerical simulation of O'Connor and Haji-Sheikh[5] is also shown in Fig. 1b. The results of the present computation agree well with the experimental data[2] and with O'Connor and Haji-Sheikh's numerical result,[5] except for the disagreement in the wall pressure near the coolant injector. In the experiment, a strong expansion wave was formed by the base of the splitter plate. However, it is obvious from Fig. 1b that such expansion waves have little effect on the cooling efficiency.

Effect of Shock Impingement on Film Cooling

Figure 2 shows comparison with the Ref. 2 experiment for shock impingement on wall pressure (Fig. 2a) and for film cooling efficiency (Fig. 2b). In Fig. 2, the shock impingement position from the splitter lip, X_{imp}, was matched to that of the experiment[2] ($X_{imp} = 14.3\ d_{inj}$) by adjusting the shock generator location. The regions where the wall pressure increases by shock impingement extend upstream for both cases. This result shows that most of the coolant flow becomes subsonic for the sonic injection. As seen in Fig. 2b, the film cooling efficiency decreased due to shock wave impingement in both the calculation and the experiment, though the degree of its decrease and the ensuing recovery due to the impingement of the expansion wave from the rear of the shock generator appear more clearly in the computation than in the experiment. Based on their experimental results, Kanda et al.[2] concluded that the decrease of the film cooling efficiency by shock impingement was caused mainly by the increase in the coolant recovery temperature due to a reduced Mach number. In this section, we attempt to confirm their conclusion and to understand in detail

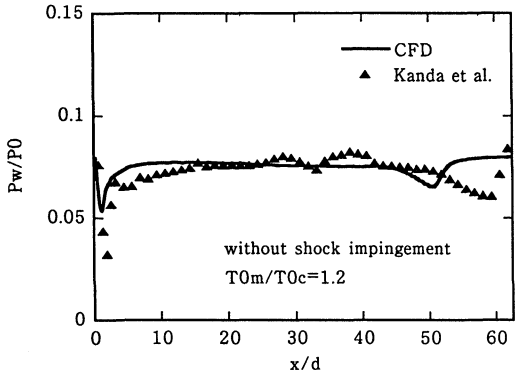

a) Wall pressure

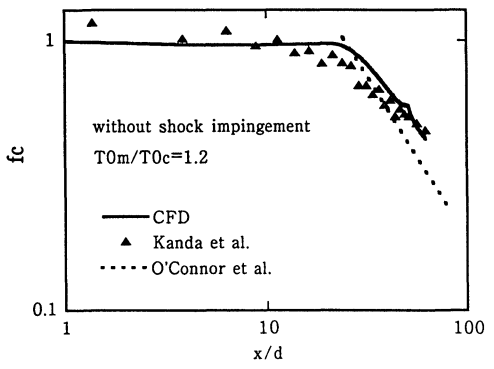

b) Film cooling efficiency

Fig. 1 Comparison of computational and experimental data without shock impingement.

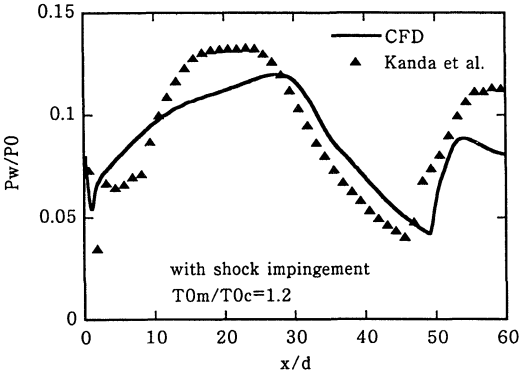

a) Wall pressure

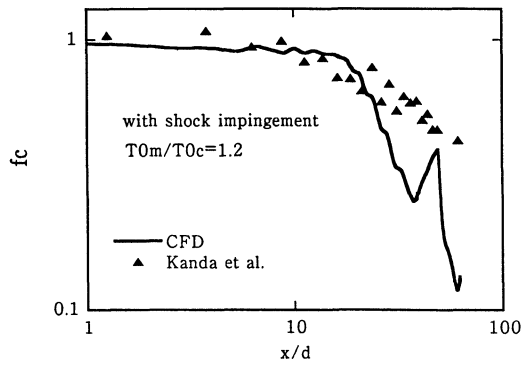

b) Film cooling efficiency

Fig. 2 Comparison of computational and experimental data with shock impingement.

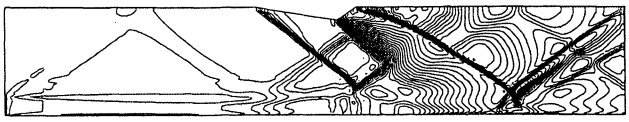

a) Pressure contour

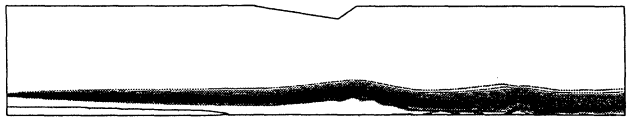

b) Contour of oxygen mole fraction for shock impingement case

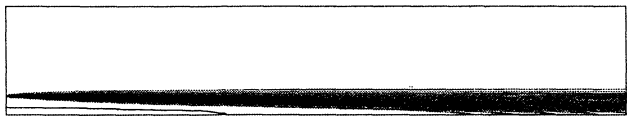

c) Contour of oxygen mole fraction for the case of no shock impingement

Fig. 3 Effect of shock impingement on mixing.

the behavior of the coolant film when shock wave impingement occurs.

Calculations were conducted for a coolant of pure nitrogen and a main flow consisting of 10% oxygen and 90% nitrogen. The layer where the oxygen concentration changes is regarded as the mixing layer of the coolant flow and the main flow. The existence of the splitter had little effect on the region where cooling efficiency decreased by the interaction with the shock wave; therefore, the splitter was not included in the calculation so as to focus on the interaction region.

Figure 3a shows the pressure contour of the flowfield where a shock wave impinges on a coolant flow. The incident shock, the expansion wave, and the recompression shock from the upper wall are clearly shown. The recompression shock reaches closer to the lower wall than the incident shock, due to acceleration of the flow by impingement of the expansion wave. Distributions of a mole fraction of oxygen are shown in Figs. 3b and 3c for the cases with and without shock impingement, respectively. As seen in Fig. 3b, the mixing layer is deflected away from the wall by the shock wave impingement and deflected back to the wall by the expansion wave impingement on the cooling film. Hyde et al.[6] reported the same tendency in their experiment. Turbulent kinetic energy increased steeply behind the position where shock wave impinged, and the value was doubled in comparison with the value at the same position in the case without shock impingement, though the impingement of the following expansion wave damps turbulence. However, turbulent kinetic energy near the wall was weak and not greatly changed by shock wave impingement. Therefore, no catastrophic change of the coolant film was observed. This result supports the earlier mentioned explanation of Kanda et al.[2] for the decrease in film cooling efficiency by shock wave impingement in their experiments.

Effect of Increase in the Injection Mach Number of a Coolant

To reduce the influence of shock impingement, supersonic injection of a coolant could be considered. Therefore, the effects of the coolant injection Mach number on the effectiveness of film cooling with shock impingement at $X_{imp}/d_{inj} = 14.3$ were investigated. Figure 4 shows the wall pressure distributions for different injection Mach numbers with same total temperature ($T_{0c} = 230$ K and $T_{0m} = 460$ K). The region where the wall pressure increases due to the interaction between a shock wave and a coolant flow is reduced with the increase in the injection Mach number of a coolant, though the maximum wall pressure increases. Figure 5 shows film cooling efficiencies for different injection Mach numbers. The degree of decrease in cooling efficiency due to shock impingement decreases when the injection Mach number increases. Also, the region where cooling efficiency unity is maintained is extended because of the reduced velocity ratio between the main flow and the coolant. Comparison of Figs. 2a and 4 suggests that the coolant

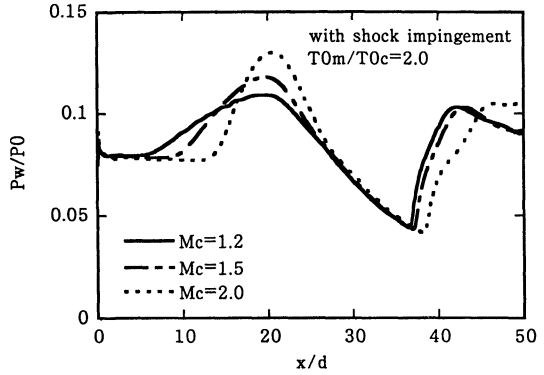

Fig. 4 Wall pressure distributions for different injection Mach numbers.

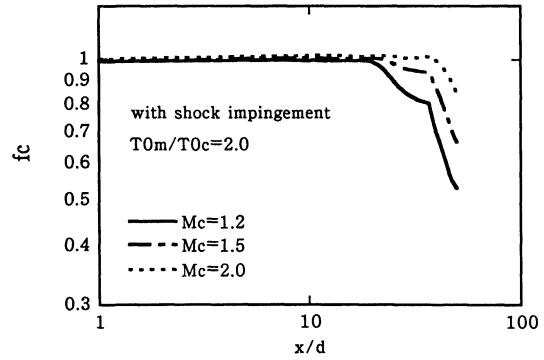

Fig. 5 Effect of injection Mach number of a coolant flow on film cooling efficiency.

Mach number of Kanda's experiment[2] might be somewhat above unity.

Conclusions

The thickness of the mixing layer of the coolant flow and of the main flow was not greatly changed by shock wave impingement, though the turbulent kinetic energy doubled behind the impingement position. This indicates that the decrease in cooling efficiency due to shock wave impingement is mainly the result of the decrease in local Mach number, as reported by Kanda et al.[2] Moreover, an increase in the injection Mach number of a coolant extended the region where film cooling is effective in the case of no shock impingement. Also, the increase in the injection Mach number mitigated the reduction of film cooling efficiency by shock wave impingement and reduced the interaction region.

References

[1]Juhany, K. A., and Hunt, M. L., "Flowfield Measurements in Supersonic Film Cooling Including the Effect of Shock-Wave Interaction," *AIAA Journal*, Vol. 32, No. 3, 1994, pp. 578–585.

[2]Kanda, T., Ono, F.,Takahashi, M., Saito, T., and Wakamatsu, Y., "Experimental Studies of Supersonic Film Cooling with Shock Wave Interaction," *AIAA Journal*, Vol. 34, No. 2, 1996, pp. 265–271.

[3]Kanda, T., and Ono, F., "Experimental Studies of Supersonic Film Cooling Shock Wave Interaction (2)," *Journal of Thermophysics and Heat Transfer*, Vol. 11, No. 4, 1997, pp. 590–593.

[4]Lam, C. K. G., and Bremhorst, K., "A Modified Form of the k-Model for Predicting Wall Turbulence," *Journal of Fluids Engineering*, Vol. 103, No. 3, 1981, pp. 456–460.

[5]O'Connor, J. P., and Haji-Sheikh, A., "Numerical Study of Film Cooling in Supersonic Flow," *AIAA Journal*, Vol. 30, No. 10, 1992, pp. 2426–2433.

[6]Hyde, C. R., Smith, B. R., Schetz, J. A., and Walker, D. A., "Turbulence Measurements for Heated Gas Slot Injection in Supersonic Flow," *AIAA Journal*, Vol. 28, No. 9, 1990, pp. 1605–1614.

T. C. Lin
Associate Editor